RESEARCH PAPER

Ferric and Ferrous Molar Ratio Effect on Physical and Magnetic Properties of Iron Oxide Nanoparticles

Sonali P. Mahaparale, Amruta R. Patil*

* patilamruta093@gmail.com, sonalimahaparale@dyppharmaakurdi.ac.in

Department of Pharmaceutical Chemistry, Dr. D. Y. Patil College of Pharmacy, Akurdi, Pune 411044, India

Abstract: Iron oxide nanoparticles have been attracted extensively due to their supermagnetic properties, preferred in biomedicine because of their biocompatibility and potential nontoxicity to human beings. Synthesis of iron nanoparticles (FeNPs) was prepared with the help of ferric chloride and ferrous sulphate by using the coprecipitation method. The variation and combination of ferric and ferrous concentrations affect the physical and magnetic properties of iron oxide nanoparticles. The effect of 0.1 M ferric and ferrous concentration on iron oxide nanoparticles was studied separately and in combination. The obtained nanoparticles were characterized by Particle size, zeta potential, Ultraviolet (UV-visible), Fourier Transform Infrared Spectroscopy (FTIR), X-ray diffraction (XRD), Scanning electron microscope (SEM), Thermal gravimetric analysis (TGA), and Vibrating-sample magnetometer (VSM) techniques. Particle size was below 200 nm and zeta potential was within the limit for all the batches. UV visible spectra at 224 nm, and FTIR exhibit two peaks at 510 and 594 cm⁻¹, indicating iron oxide NPs and XRD confirmed the crystalline nature of Fe. SEM showed a spherical shape for all batches. The use of a combination of ferric and ferrous is more effective than its individual use. TGA and VSM studies confirmed its magnetic properties.

Keywords: Ferric chloride, Ferrous sulphate, Iron oxide, Supermagnetic, Magnetic nanoparticles.

1. INTRODUCTION

In recent years, the exploration of nanomaterials has surged, driven by their unique properties and versatile applications in various scientific domains. Among these nanomaterials, iron oxide nanoparticles have garnered significant attention, owing to their unique magnetic and catalytic properties [1].

In recent times, iron oxide nanoparticles (IONPs) have captivated the scientific community, drawing significant attention owing to their extraordinary attributes. These nanoparticles boast distinctive features, including superparamagnetism, an impressive surface-to-volume ratio, substantial surface area, and a straightforward separation methodology. These inherent qualities have propelled IONPs to the forefront of research interest, unlocking diverse possibilities for applications across multiple disciplines. From biomedical applications, including drug delivery and imaging, to environmental remediation and catalysis [2]. The synthesis of IONPs is achieved through a judicious selection of established and innovative methods. Chemical methods, involving the controlled precipitation of iron salts in the presence of stabilizing agents, are employed to create nanoparticles with precise control over size and morphology. The co-precipitation technique, where iron salts are simultaneously precipitated in an alkaline medium, stands out for its simplicity and scalability. Thermal decomposition methods are harnessed for their ability to yield monodisperse IONPs. This involves the controlled decomposition of iron-containing precursors at elevated temperatures, resulting in nanoparticles with well-defined sizes and superior crystallinity. The high-temperature pyrolysis ensures the formation of homogeneous nanoparticles with minimal agglomeration [3].

Iron oxide, a compound composed of iron and oxygen, exists in various forms, each with distinct properties and applications. The most common forms include: Iron (II) oxide (FeO), Iron (III) oxide (Fe_2O_3), Magnetite (Fe_3O_4), Goethite (FeO(OH)), Maghemite (Υ-Fe_2O_3), Hematite (α-Fe_2O_3) [4]. Among iron oxides; γ-Fe_2O_3 and Fe_3O_4 are widely used materials [5]. The magnetic properties of magnetite nanoparticles exhibit a notable dependency on the concentration of manganese ions in both $FeSO_4$ and $FeCl_3$ reactants. Specifically, when adopting a 1:1 stoichiometric ratio of ferrous to ferric ions (Fs: Fc), it becomes evident that nanoparticles with higher manganese ion concentrations

demonstrate a discernibly greater saturation magnetization compared to their counterparts with lower manganese concentrations. This highlights the significant impact of manganese ion incorporation during the synthesis process on the magnetic behavior of the resulting magnetite nanoparticles [6]. The concentration of ferric chloride solution affects the properties of IONPs [7]. In the present study, IONPs were synthesized by using the coprecipitation method [8] by using ferric chloride [9, 10], ferric sulphate [5] and ammonia. [11]

2. EXPERIMENTAL PROCEDURES

2.1. Materials

For the synthesis of IONPs in this study, Ferric chloride Hexahydrate, Ferrous sulphate, and 25% Ammonia solution were used. Ferrous sulphate and 25% Ammonia solution were procured from AnaLab Fine Chemicals, Mumbai and Ferric chloride Hexahydrate was procured from Loba Chemie Pvt Ltd. All these chemicals are of AR grade and used with unprocessed purification.

2.2. Synthesis and Optimization of IONPs

Firstly, IONPs were synthesized by using the coprecipitation method with four different concentrations of 0.01, 0.04, 0.07, and 0.1 M of Ferric chloride coded as M1, M2, M3 and M4 respectively at 80°C & pH 10 for 2 hours. Then optimized batch of IONPs with Ferric chloride, with the same concentration batch with ferrous sulphate were synthesized separately and in combination and coded as FM1, FM2 and FM3 respectively.

2.3. Characterization of IONPs

FTIR (Bruker alpha II) spectroscopy was used to determine the presence of functional groups in IONPs between the range of 4000-400 cm^{-1}. UV-visible spectroscopy (Shimadzu) operated in a wavelength range of 200-400nm to examine and confirm the formation of IONPs by absorbance. The shape and morphology of IONPs were examined by using SEM (ShimadzuSSX-550). The particle size distribution and zeta potential were measured using Horiba Scientific. The structure and nature of IONPs were examined by XRD in the 2θ range of 20-90°. TGA analysis was completed for all batches in a nitrogen atmosphere with a heating rate of 10°c/min. The

magnetization measurements were measured by using VSM at room temperature.

3. RESULTS AND DISCUSSION

FTIR spectrum analysis indicated the presence of IONPs. The peak in Fig. 1, between 620.96 to 692.18 to 714.50 relates to the Fe-O group. It indicates the formation of IONPs [12]. Two more bands near at 3300 and 1600 due to H_2O molecules. The rest of the bands near 3500 are due to the OH bond and other bands near 700, and 1000 are due to iron oxide on the surface of IONPs [13].

The UV-visible spectra were used to identify the IONPs. The absorption spectra were found at 227 nm and absorbance was measured and it was 1.179, 0.079, 1.105, 0.256, 0.232, 0.352 for M1, M2, M3, M4/FM1, FM2 and FM3 respectively [14] as shown in Table 1. With an increase or decrease in the concentration of solution, the intensity of peaks was also changed.

The irregular shapes were observed in Fig. 2, some are spherical due to the agglomeration process in all the batches except FM3 due to some agglomeration [14]. For the FM3 batch i.e. when we used the $FeCl_2$ and $FeSO_4$ in combination, all particles are uniformly spherical.

The variation in particle size of IONPs with different concentrations of Ferric chloride is shown in Table 1 and Fig. 3. When ferric chloride and ferrous sulphate were used in combination, the particle size was slightly increased. The particle size of 0.1 M ferric chloride is smaller than 0.1 M ferrous sulphate, due to alteration in the surface area-to-volume ratio [6].

The stability of nanoparticles (NPs) can be effectively assessed through their zeta potential. We found that all batches exhibit zeta potential within the range of -11.1 to -9.1 mv in Fig. 4, indicating the stable state of NPs [15]. As the concentration of ferric chloride increases, the zeta potential slightly shifted, as they were synthesized at the same pH. The zeta potential value of IONPs by using 0.1 M ferric chloride and 0.1 M $FeSO_4$ were near to each other and when they were used in combination with .1 M ferric chloride and 0.1 M $FeSO_4$ for IONPs, the value was near to both.

Fig. 5 shows the XRD patterns of the synthesized MNPs at increasing molarities for M1 to M4 and FM1 to FM4, respectively.
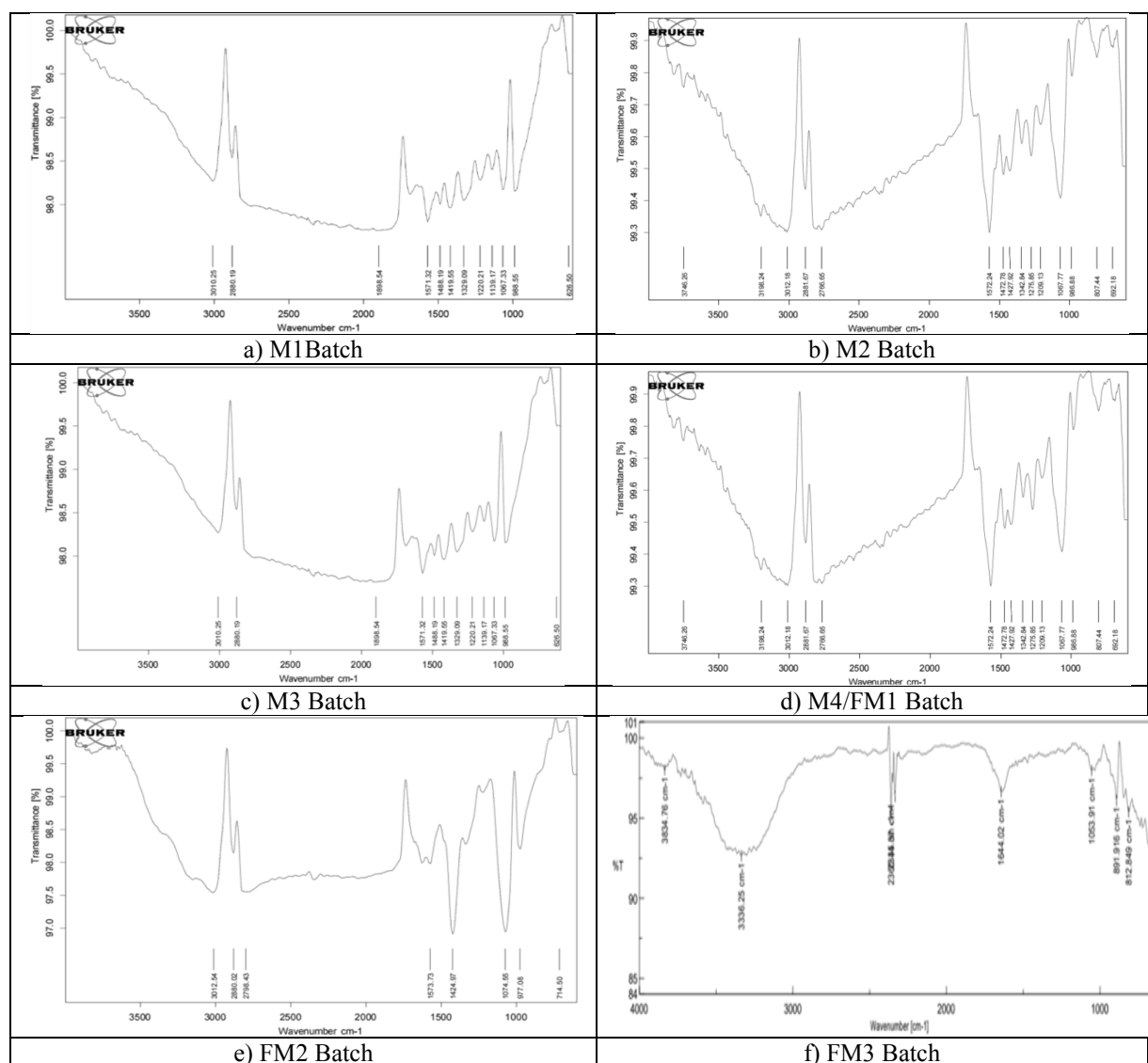
a) M1Batch

b) M2 Batch

c) M3 Batch

d) M4/FM1 Batch

e) FM2 Batch

f) FM3 Batch

Fig. 1. IR spectra of IONPs for all the batches.

Table 1. Particle size, zeta potential and UV absorbance of IONPs batches.

Batch No	Mean Particle size of IONPs (nm)	Zeta Potential (mv)	UV Absorbance	Batch No	Mean Particle size of IONPs (nm)	Zeta Potential (mv)	UV Absorbance
M1	115.7	-9.2	0.079	M4/FM1	83.7	-10.9	0.256
M2	118.4	-9.1	0.089	FM2	105.9	-10.7	0.232
M3	157.4	-11.1	0.105	FM3	115.7	-10.1	0.252

The data shows diffraction peaks at 2θ, near 30°, 35°, 44°, 57°, and 63° which can be indexed to the planes of Fe_2O_3 in a cubic phase [16]. It indicates the crystalline nature of IONPs in all batches. As compared to other batches, there are sharp and clear peaks in the FM3 batch indicating more crystalline and revealing the formation of ϒ and $α\text{-}Fe_2O_3$ [14]. TGA is a versatile analytical technique with

applications ranging from the identification of nanoparticle composition to the assessment of thermal and oxidative stability. The decomposition of metal oxide nanoparticles in a thermogravimetric analysis (TGA) can indeed occur in one or more stages, depending on the specific characteristics of the nanoparticles and the nature of the metal oxide [17].
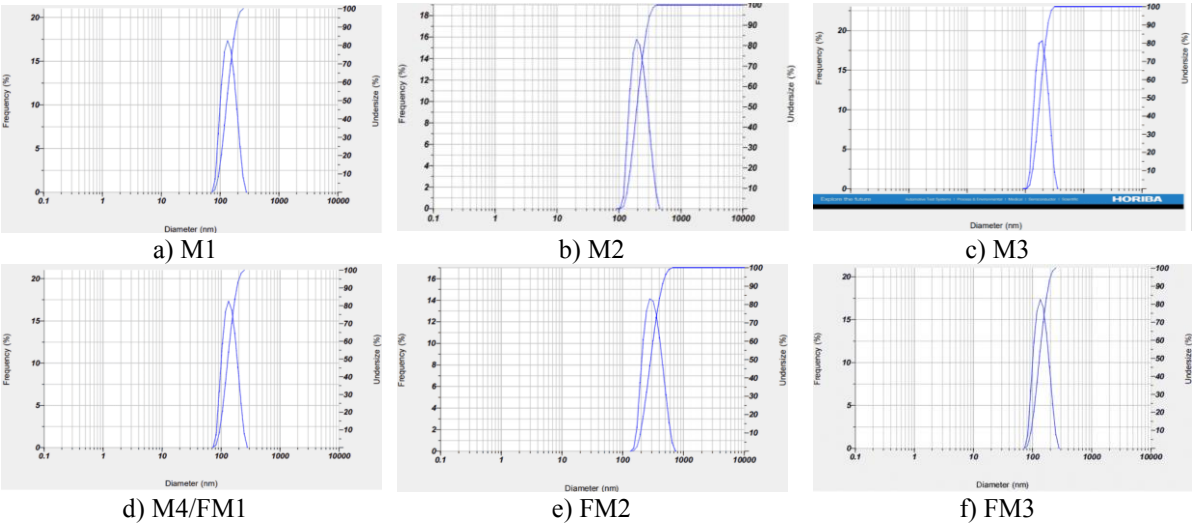
3

Amruta R. Patil et al.

a) M1

b) M2

c) M3

d) M4/FM1

e) FM2

f) FM3

Fig. 2. SEM Images of IONPs batches.

a) M1

b) M2

c) M3

d) M4/FM1

e) FM2

f) FM3

Fig. 3. Particle size of IONPs.

4

a) M1   b) M2   c) M3

d) M4/FM1   e) FM2   f) FM3

Fig. 4. Zeta Potential of IONPs.

a) M1   b) M2

c) M3   d) M1/FM1

e) FM2   f) FM3

Fig. 5. XRD Pattern of IONPs.

There is continuous weight loss in three stages as shown in figure 6, during 1st stage of 25-150°C, weight loss is due to the removal of water content along with some hydrophilic compounds from the surface of IONPs. In 2nd stage of 150°C-400°C, weight loss is due to organic molecules. Beyond 400°C, weight loss is due to the presence of IONPs [18].

The magnetic behavior of the IONPs was examined by VSM at room temperature.

a) M1   b) M2   c) M3

d) M4/FM1   e) FM2   f) FM3

Fig. 6. TGA Profile of IONPs batches.

a) M1   b) M2   c) M3

d) M4/FM1   e) FM2   f) FM3

Fig. 7. VSM of IONPs.

The saturation magnetization were 2.82 emu/g, 7.2 emu/g, 2.08 emu/g, 3.77 emu/g, 91.82 emu/g, 72.05 emu/g for M1, M2, M3, M4/FM1, FM2, FM3 batch respectively as shown in figure 7. The magnetization curves are characteristic of superparamagnetic nanoparticles and demonstrate that the magnetic properties of the nanoparticles for all the batches [19]. Magnetization saturation was high when we used ferrous sulphate [6] but in combination with ferric chloride, it was reduced.

4. CONCLUSIONS

In conclusion, the study successfully synthesized and characterized IONPs with a detailed analysis of their structural, morphological, and magnetic properties. The variations in properties were linked to different concentrations of Ferric chloride and the use of Ferrous sulphate, providing insights into the influence of these parameters on the characteristics of the synthesized IONPs. First, IONPs were synthesized by using different concentrations of ferric chloride and the optimized batch with 0.1 M concentration was based on different

6

characterization techniques. Then, the combination and separate entity of Ferric chloride and ferrous sulphate were used to form IONPs. When we used $FeCl_2$ and $FeSO_4$ in combination, it had a more uniform size, shape, crystalline nature, stable and high magnetization value. By pursuing these future scopes, researchers can contribute to the advancement of knowledge in nanotechnology and harness the unique properties of IONPs for a wide range of practical applications in medicine, catalysis, environmental remediation, and beyond.

CONFLICT OF INTEREST

There are no conflicts to declare including any competing financial interest.

REFERENCES

[1]. Singh, K., Chopra, D.S., Singh, D. and Singh, N.,. "Optimization and ecofriendly synthesis of iron oxide nanoparticles as potential antioxidant". Arabian Journal of Chemistry, 2020, 13(12), 9034-9046. 10.1016/j.arabjc.2020.10.025.

[2]. Ali, A., Zafar, H., Zia, M., ul Haq, I., Phull, A.R., Ali, J.S. and Hussain, A., "Synthesis, characterization, applications, and challenges of iron oxide nanoparticles". Nanotechnology, science and applications, 2016, 9, 49-67. 10.2147%2FNSA.S99986.

[3]. Vargas-Ortiz, J.R., Gonzalez, C. and Esquivel, K., "Magnetic Iron Nanoparticles: Synthesis, Surface Enhancements, and Biological Challenges". Processes, 2022, 10(11), 1-29. 10.3390/pr10112282.

[4]. Lakshmanan, P. K., Vignesh, K. and Karthikeyan N., "Applications and Toxicology of Iron Oxide Nanoparticles. Iron Ores and Iron Oxides - New Perspectives". IntechOpen. 2023, 1, 1-14. 10.5772/intechopen.1001336.

[5]. Ajinkya N., Yu X., Kaithal P., Luo H., Somani P., Ramakrishna S. "Magnetic Iron Oxide Nanoparticle (IONP),. Synthesis to Applications: Present and Future". Materials (Basel). 2020, 13(20), 1-35. 10.3390/ma13204644.

[6]. Mazrouaa, A.M., Mohamed, M.G. and Fekry, M., "Physical and magnetic properties of iron oxide nanoparticles with a different molar ratio of ferrous and ferric". Egyptian Journal of Petroleum, 2019, 28(2), 165-171. 10.1016/j.ejpe.2019.02.002.

[7]. Chen, A., Wang, H., Li, X., "Influence of concentration of $FeCl_3$ solution on properties of polypyrrole–Fe_3O_4 composites prepared by common ion absorption effect". Synthetic Metals, 2004, 2 (3), 153-157. 10.1016/j.synthmet.2004.04.018.

[8]. LaGrow, A.P., Besenhard, M.O., Hodzic, A., Sergides, A., Bogart, L.K., Gavriilidis, A. and Thanh, N.T.K., "Unravelling the growth mechanism of the co-precipitation of iron oxide nanoparticles with the aid of synchrotron X-Ray diffraction in solution". Nanoscale, 2019, 11(14), 6620-6628. 10.1039/D3NR05589B.

[9]. Bouafia, A. and Laouini, S.E. "Green synthesis of iron oxide nanoparticles by aqueous leaves extract of Mentha Pulegium L.: Effect of ferric chloride concentration on the type of product". Materials Letters, 2020, 265, 127364. 10.1016/j.matlet.2020.127364

[10]. Bouafia, A., Laouini, S.E., Khelef, A., Tedjani, M.L. and Guemari, F., "Effect of ferric chloride concentration on the type of magnetite (Fe_3O_4) nanoparticles biosynthesized by aqueous leaves extract of Artemisia and assessment of their antioxidant activities". Journal of Cluster Science, 2021, 32(1), 1033-1041. 10.1007/s10876-020-01868-7

[11]. Saleh, R., Prakoso, D. P., Prakoso, S. P., "Preparation And Characterization Of Iron Oxide Nanoparticles For Application In Biomedicine". Indonesian Journal of Material Science, 2009, 1(1), 61-66. 273771024.

[12]. Nosrati, H., Sefidi, N., Sharafi, A., Danafar, H. and Manjili, H.K., "Bovine Serum Albumin (BSA) coated iron oxide magnetic nanoparticles as biocompatible carriers for curcumin-anticancer drug". Bioorganic chemistry, 2018, 76, 501-509. 10.1016/j.bioorg.2017.12.033

[13]. Villegas, V.A.R., Ramírez, J.I.D.L., Guevara, E.H., Sicairos, S.P., Ayala, L.A.H. and Sanchez, B.L., "Synthesis and characterization of magnetite nanoparticles

for photocatalysis of nitrobenzene". Journal of Saudi Chemical Society, 2020, 24(2), 223-235. 10.1016/j.jscs.2019.12.004

[14]. Takai, Z.I., Mustafa, M.K., Asman, S. and Sekak, K.A., "Preparation and characterization of magnetite (Fe$_3$O$_4$) nanoparticles by sol-gel method". Int. J. Nanoelectron. Mater, 2019, 12, 37-46.

[15]. Chandrasekar, N., Kumar, K., Balasubramanian, K.S., Karunamurthy, K. And VARADHARAJAN, R., "Facile Synthesis Of Iron Oxide, Iron-Cobalt And Zero Valent Iron Nanoparticles And Evaluation Of Their Anti Microbial Activity, Free Radicle Scavenging Activity And Antioxidant Assay". Digest Journal Of Nanomaterials & Biostructures (DJNB), 2013, 8(2), 99. 765-775.

[16]. Mishra, A. and Sardar, M., "Isolation of genomic DNA by silane-modified iron oxide nanoparticles". Nanotechnology: Novel Perspectives and Prospects, 2015, 309-315.

[17]. Rami, J.M., Patel, C.D., Patel, C.M. and Patel, M.V., "Thermogravimetric analysis (TGA) of some synthesized metal oxide nanoparticles". Materials Today: Proceedings, 2021, 43, 655-659. 10.1016/j.matpr.2020.12.554

[18]. Karade, V.C., Dongale, T.D., Sahoo, S.C., Kollu, P., Chougale, A.D., Patil, P.S. and Patil, P.B., "Effect of reaction time on structural and magnetic properties of green-synthesized magnetic nanoparticles". Journal of Physics and Chemistry of Solids, 2018, 120, 161-166. 10.1016/j.jpcs.2018.04.040.

[19]. Basly, B., Felder-Flesch, D., Perriat, P., Billotey, C., Taleb, J., Pourroy, G. and Begin-Colin, S., "Dendronized iron oxide nanoparticles as contrast agents for MRI". Chemical Communications, 2010, 46(6), 985-987.

[20]. Attia, N.F., Abd El-Monaem, E.M., El-Aqapa, H.G., Elashery, S.E., Eltaweil, A.S., El Kady, M., Khalifa, S.A., Hawash, H.B. and El-Seedi, H.R., "Iron oxide nanoparticles and their pharmaceutical applications". Applied Surface Science Advances, 2022, 11, 100284. 1-14. 10.1016/j.apsadv.2022.100284.

[21]. Fatima, H., Lee, D.W., Yun, H.J. and Kim, K.S., "Shape-controlled synthesis of magnetic Fe$_3$O$_4$ nanoparticles with different iron precursors and capping agents". RSC advances, 2018, 8(41), 22917-22923. 10.1021/acsomega.0c02928.

[22]. Al-Hakkani, M.F., Gouda, G.A. and Hassan, S.H., "A review of green methods for phyto-fabrication of hematite (α-Fe$_2$O$_3$) nanoparticles and their characterization, properties, and applications". Heliyon, 2020, 7(1), 1-16. 10.1016/j.heliyon.2020.e05806.

[23]. Saleh R., Prakoso D.P, Prakoso S.P., "Preparation And Characterization Of Iron Oxide Nanoparticles For Application In Biomedicine". Indonesian Journal of Materials Science, 2009, 61-66.

8